Accepted Manuscript

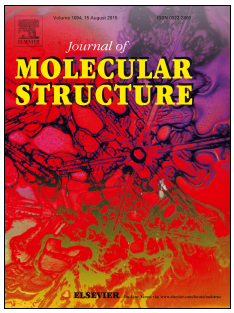

Study of an efficient conversion of 1,3-dimethyl-5-(Arylazo)-6-Amino-Uracils to 1,3-dimethyl-8-(Aryl)-Azapurin-2,6-Diones

Diptanu Debnath, Atanu Purkayastha, Alexander Kirillov, Rakesh Ganguly, Tarun Kumar Misra

PII: S0022-2860(17)31167-5

DOI: 10.1016/j.molstruc.2017.08.087

Reference: MOLSTR 24225

To appear in: *Journal of Molecular Structure*

Received Date: 9 May 2017

Revised Date: 25 August 2017

Accepted Date: 26 August 2017

Please cite this article as: D. Debnath, A. Purkayastha, A. Kirillov, R. Ganguly, T.K. Misra, Study of an efficient conversion of 1,3-dimethyl-5-(Arylazo)-6-Amino-Uracils to 1,3-dimethyl-8-(Aryl)-Azapurin-2,6-Diones, *Journal of Molecular Structure* (2017), doi: 10.1016/j.molstruc.2017.08.087.

Study of an Efficient Conversion of 1,3-Dimethyl-5-(Arylazo)-6-Amino-Uracils to 1,3-Dimethyl-8-(Aryl)-Azapurin-2,6-Diones

Diptanu Debnath, Atanu Purkayastha, Alexander Kirillov, Rakesh Ganguly and Tarun Kumar Misra

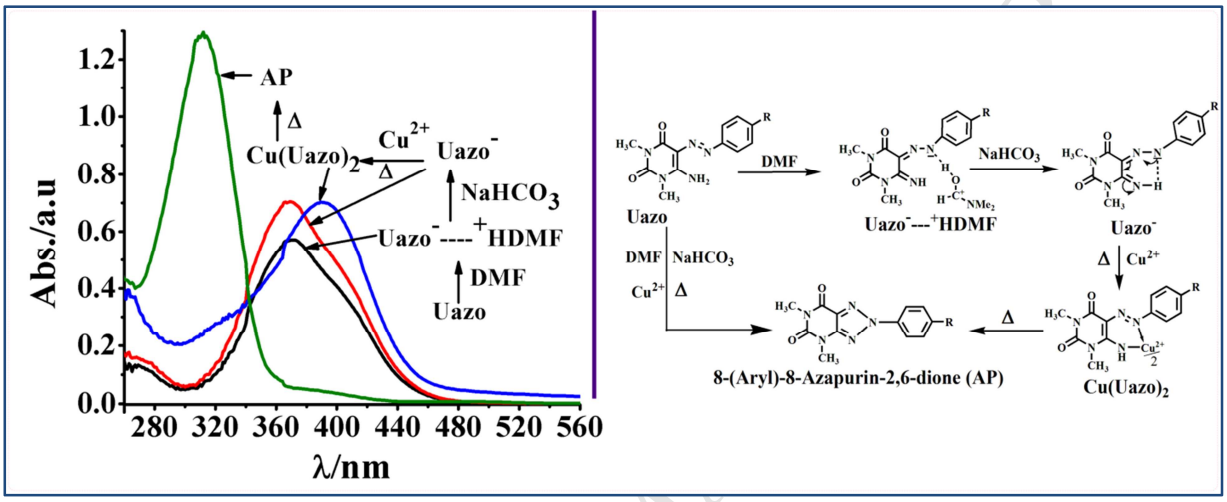

1,3-Dimethyl-5-(arylazo)-6-amino-uracils are converted to 1,3-dimethyl-8-(aryl)-azapurin-2,6-dione under modified alkaline copper(II)-oxidation method.

Study of an Efficient Conversion of 1,3-Dimethyl-5-(Arylazo)-6-Amino-Uracils to 1,3-Dimethyl-8-(Aryl)-Azapurin-2,6-Diones

Diptanu Debnath[a], Atanu Purkayastha[a], Alexander Kirillov[b*], Rakesh Ganguly[c*] and Tarun Kumar Misra[a*]

[a]*Department of Chemistry, National Institute of Technology, Agartala 799046, Tripura, India*

[b]*Instituto Superior Técnico, University of Lisbon, Lisbon 1049001, Portugal*

[c]*Division of Chemistry & Biological Chemistry, Nanyang Technology University, Singapore 639798*

***Corresponding Authors:** E-mail: [a]tkmisra70@yahoo.com; [b]kirillov@tecnico.ulisboa.pt; [c]rganguly@ntu.edu.sg; Tel.: +91-381-2346630; Fax: +91-381-2346360.

Abstract

6-Aminouracils have extensively been used as precursors for synthesizing numerous uracil derivatives of biological and pharmaceutical significance. This study describes an application of 1,3-dimethyl-5-(arylazo)-6-aminouracils (Uazo: Uazo1-Uazo4, precursors) for an efficient synthesis of a series of 8-substituted-azapurins (AP), namely 1,3-dimethyl-8-(aryl)-azapurin-2,6-diones (aryl = *p*-HC_6H_4 (**AP1**), -MeC_6H_4 (**AP2**), -ClC_6H_4 (**AP3**), and -$SO_2NH_2C_6H_4$ (**AP4**)) following an oxidation method in the presence of copper(II) nitrate and in alkaline medium. The obtained compounds were isolated in good yields as crystalline air-stable products and have been fully characterized in the solution by UV-vis and NMR spectroscopy, as well as in the solid state by FT-IR spectroscopy, elemental analysis, and single-crystal X-ray diffraction (for **AP2** and **AP4**). UV-vis study evidences that the conversion of the 6-aminouracil precursors occurs *via* an intermediate, Cu(II)-complex and a plausible mechanism for the formation of **AP1**-**AP4** has been proposed. Unlike **AP2** the crystal structure of **AP4** reveals the formation of interdigitated 1D H-bonded chains that has been topologically classified within the 2C1 type. The ^{1}H NMR spectra of the products have proton signals that completely devoid of hydrazone (–NH–) and imine (=NH) signals of their parent Uazo derivatives, thus confirming their full conversion and a stability of the **AP1**-**AP4** in solution. The excitation and emission spectra of **AP1**-**AP4** were also recorded in solution, revealing electronic transitions between similar vibrational energy levels of S_0 (singlet ground state) and S_1 (singlet first excited state).

Keywords: Organic synthesis, Aminouracils, Azapurins, Spectroscopic characterization, Crystal structures.

1. Introduction

Purine (adenine and guanine) and pyrimidine (cytosine, thymine, and uracil) bases are the two different important hydrolysis products of nucleic acids. These bases have widely been studied from diverse perspectives, particularly their interactions with metals and chemical modification [1-16], aiming at understanding in their *vivo* functioning and tuning pharmacological behavior. Chemical modification of natural nucleobases (*i.e.*, purines and pyrimidine bases) in search of new drugs for effective antiviral and antitumour therapy has extensively been explored [4-16]. In particular, the modification in purines (see Scheme 1(A)) has generally been accomplished at its imidazole ring, resulting in the substitution of CH by N in position 8 of the purine ring and forming 8-azapurines [6-8] (see Scheme 1(B)). Such a conversion of purines to 8-azapurines leads to an effective decrease of the electron density at this position [17] and thus can significantly influence their chemical and biological properties [18], including their recognized activity as anti-tumour drugs [18a]. Moreover, 8-azapurine family includes 8-azaadenines (6-amino-8-azapurine), 8-azaguanines (2-amino-8-azapurin-6-one), 8-azainosine (9-β-D-ribofuranosyl-8-azapurin-6-one), 8-azahypoxanthines (8-aza-purin-6-one), and 8-azaxanthines (8-azapurin-2,6-dione, Scheme 1C), which differ from each other by the presence of amino and/or hydroxyl substituents in the positions 2 and 6 [9,19].

(Scheme 1)

The present work deals with the derivatives of 1,3-dimethyl-8-azapurin-2,6-dione (Scheme 1D). The synthesis of 8-azapurine derivatives generally starts with the starting materials based on either pyrimidine or 1,2,3-triazole derivatives. The first of 8-azapurines, 1,3-dimethyl-8-azapurin-2,6-dione (Scheme 1D), was made by Traube [20] *via* cyclization of the corresponding 4,5-diaminopyrimidine with nitrous acid. Later on, the Traube synthesis has proved to be compatible with many kinds of groups in the starting pyrimidine moiety for synthesizing 8-azapurines [21-24]. The mobile hydrogen atom at the 8-position in 1,3-dimethyl-8-azapurin-2,6-dione (Scheme 1D) can, theoretically, be attached to any one of the three triazole-nitrogen atoms, giving the possibility to synthesize different N-substituted derivatives. A notable deficiency of the Traube synthesis concerns its inability to produce 7- or 8- substituted 8-azapurines starting from aminopyrimidine derivatives [25, 26] and such difficulty could be overcome using triazole

derivatives [27]. It is noteworthy to mention that the bond arrangement in 8-azapurine (Scheme 1B) might suggest instability.

Nevertheless, the 6-aminouracils are extensively used as precursors for synthesizing numerous uracil derivatives of biological and pharmaceutical importance [28-30]. For example, Sulfadimethoxine [30], a sulphanilamide or sulfa-drug, is prepared from 6-aminouracil and is used to inhibit the uracil-DNA glycosylase [31] and the dihydropyrimidine dehydrogenase enzymes [32]. Our laboratory has been engaged in synthesizing 5-(arylazo)-6-aminouracils and exploring their chemistry [33]. From literature it is found that there are several effective methods [34, 35] converting 2-amino-azo compounds to 2-substituted v-triazole derivatives; these are heating, chromic acid oxidation, lead tetraacetate oxidation, oxidation with alkaline copper sulfate, and oxidation with copper sulfate in pyridine-water. In particular, Islam and Nagamatsu [36] demonstrated the synthesis of some derivatives of 1,3-dimethyl-8-(aryl)azapurin-2,6-diones *via* the oxidation with copper sulfate in pyridine-water medium.

Inspired by these results and following our general interest in this area of synthetic organic chemistry, we report in the present study an efficient conversion of a series of 1,3-dimethyl-5-(arylazo)-6-aminouracils (Uazo1-Uazo4) to 1,3-dimethyl-8-(aryl)azapurin-2,6-diones (**AP1**-**AP4**), by applying a procedure for the oxidation with alkaline copper nitrate in DMF-water mixture. As a base, $NaHCO_3$ was used. The present report thus includes the synthesis, full characterization, and detailed spectroscopic studies of the **AP1**-**AP4** products, crystal structures of **AP2** and **AP4**, as well as a topological analysis of the identified 1D H-bonded network in the crystal packing pattern of **AP4**. The sulfonamide derivative, in particular, can potentially constitute a promising pharmaceutically active agent, as the sulfonamide ($-SO_2NH_2$) group is an integral part of various sulfa-drugs [37-39]. In addition, the molecules containing sulfonamide functionality can exhibit interesting solid state properties [40-44].

2. Experimental

2.1. Materials and instruments

All chemicals were commercially available (reagent grade) and were used without any further purification. All solvents were of A. R. grade. 1,3-Dimethyl-6-aminouracil and 1,3-dimethyl-5-(arylazo)-6-aminouracil were prepared following reported procedures [33].

Melting points were determined on a Labtech Digital melting point apparatus with a heating rate of 2 °C/min and not corrected. IR spectra were recorded on a Perkin Elmer FT-IR spectrophotometer (model RX-1) in the region 4000–400 cm^{-1} (KBr pellets). The ^{1}H NMR and ^{13}C NMR spectra in DMSO-D_6 were recorded on a JEOL DELTA2 spectrometer at 500 MHz and 125 MHz, respectively. The electronic spectra were recorded on a Shimadzu UV-*vis*-1800 spectrophotometer. Excitation and emission spectra of all the compounds were recorded on a Perkin Elmer LS 55 Fluorescence Spectrometer. Excitation and emission slits were set to 10 and 2.5 nm. Elemental analyses were made on a Perkin Elmer 2400 series-II analyzer and the obtained results are in good agreement with the calculated values.

*2.2. Synthesis of 1,3-dimethyl-8-(aryl)-azapurin-2,6-dione derivatives (**AP1**-**AP4**)*

General procedure. The compounds **AP1**-**AP4** were synthesized *via* an alkaline copper sulfate method [34] with some modifications. Typically, 1,3-dimethyl-5-(phenylazo)-6-aminouracil (Uazo1, 103.6 mg, 0.4 mmol) was dissolved in DMF, followed by the addition of an aqueous solution of $NaHCO_3$ (33.6 mg, 0.4 mmol). The obtained mixture was heated at 70 ^{o}C with continuous stirring over 20 minutes. Then, to this warm mixture a DMF solution of $Cu(NO_3)_2 \cdot 3H_2O$ (48.4 mg, 0.2 mmol) was added slowly with continuous stirring for further 1 h at the same temperature. An intense yellow powder of the product started to precipitate in the course of cooling the reaction mixture down to room temperature. The product was filtered off, washed with water, and dried in vacuum. X-ray quality single crystals can be obtained by re-dissolving the product in DMF-water (3:1 v/v) mixture, followed by slow evaporation for two weeks. Single crystals of **AP2** and **AP4** were analyzed for molecular structure of the products.

Physical and spectral data of the obtained products are given as follows.

*1,3-dimethyl-8-(phenyl)-azapurin-2,6-dione (**AP1**)*

Yellow square-plate crystals (yield: 53%) with a melting point of 265±1 °C. FT-IR (KBr pellet, υ/cm^{-1}): 2817 (bw, Ar-H), 1726, 1676 (s, >C=O), 1606, 1592 (bs, >C=N-), 1493 (sw, -C-

C), 1384, 1351, 1295 (s, -N-C), 1061 (s, -N-N), 990, 961, 764, 744, 692, and 652 (other bands). ^{1}H NMR (DMSO-D_6, δ/ppm): 8.08–8.06 (d, 2H, Ar-H), 7.64–7.49 (m, 3H, Ar-H), 3.49 (s, 3H, N(3)-CH_3), and 3.28 (s, 3H, N(1)-CH_3). ^{13}C NMR (125 MHz, DMSO-D_6, δ/ppm): 155.91 (>C=O), 155.77 (>C=O), 150.74 (>C=N), 150.06 (>C=N), 138.54 (Ar-C), 131.40 (Ar-C), 129.91 (Ar-C), 129.04 (Ar-C), 126.68 (Ar-C), 118.89 (Ar-C), 30.80 (N-CH_3), 28.17 (N-CH_3). Anal. Calcd. for $C_{12}H_{11}N_5O_2$: C, 56.03; H, 4.31; N, 27.22, Found: C, 56.12; H, 4.26; N, 27.02.

*1,3-dimethyl-8-(p-Me-phenyl)-azapurin-2,6-dione (**AP2**)*

Yellow square-plate crystals (yield: 58%) with a melting point of 271±1 °C. FT-IR (KBr pellet, υ/cm^{-1}): 2822 (bw, Ar-H), 1726, 1677 (s, >C=O), 1595 (bs, >C=N-), 1508 (sw, -C-C), 1384, 1353, 1297 (s, -N-C), 1054 (s, -N-N), 989, 977, 775, and 747(other bands). ^{1}H NMR (DMSO-D_6, δ/ppm): 7.95-7.39 (dd, 4H, Ar-H), 3.47 (s, 3H, N(3)-CH_3), 3.27 (s, 3H, N(1)-CH_3), and 2.37 (s, 3H, Ar-CH_3). ^{13}C NMR (125 MHz, DMSO-D_6, δ/ppm): 155.95 (>C=O), 155.81 (>C=O), 150.79 (>C=N), 150.01 (>C=N), 138.90 (Ar-C), 136.45 (Ar-C), 130.28 (Ar-C), 126.39 (Ar-C), 125.67 (Ar-C), 118.84 (Ar-C), 30.81 (N-CH_3), 28.18 (N-CH_3), and 20.58 (Ar-CH_3). Anal. Calcd. for $C_{13}H_{13}N_5O_2$: C, 57.56; H, 4.83; N, 25.82, Found: C, 57.51; H, 4.52; N, 25.89.

*1,3-dimethyl-8-(p-Cl-phenyl)-azapurin-2,6-dione (**AP3**)*

Yellow square-plate crystals (yield: 61%) with a melting point of 261±1 °C. FT-IR (KBr pellet, υ/cm^{-1}): 2830 (bw, Ar-H), 1717, 1683 (s, >C=O), 1608 (bs, >C=N-), 1493 (sw, -C-C), 1384, 1351, 1292 (s, -N-C), 1091, 1054 (s, -N-N), 965, 776, and 744 (other bands). ^{1}H NMR (DMSO-D_6, δ/ppm): 8.10-7.67 (dd, 4H, Ar-H), 3.49 (s, 3H, N(3)-CH_3) and 3.28 (s, 3H, N(1)-CH_3). ^{13}C NMR (125 MHz, DMSO-D_6, δ/ppm): 155.68 (>C=O), 150.70 (>C=N), 150.16 (>C=N), 137.29 (Ar-C), 133.32 (Ar-C), 129.90 (Ar-C), 127.01 (Ar-C), 120.59 (Ar-C), 30.79 (N-CH_3), 28.18 (N-CH_3). Anal. Calcd. for $C_{12}H_{10}ClN_5O_2$: C, 49.41; H, 3.46; N, 24.01, Found: C, 50.01; H, 3.59; N, 23.92.

*1,3-dimethyl-8-(p-SO_2NH_2-phenyl)-azapurin-2,6-dione (**AP4**)*

Yellow square-plate crystals (yield: 55%) with a melting point of 248±1 °C. FT-IR (KBr pellet, υ/cm^{-1}): 2924 (bw, Ar-H), 1725, 1669 (s, >C=O), 1609, 1590 (bs, >C=N-), 1494 (sw, -C-C), 1384, 1351, 1299 (s, -N-C), 1161 (s, >S=O),1096, 1055 (s, -N-N), 958, 856, 775, 744, 647,

and 551 (other bands); ^{1}H NMR (DMSO-D_6, δ/ppm): 8.27–8.02 (dd, 4H, Ar-H), 7.52 (s, -SO_2NH_2), 3.49 (s, 3H, N(3)-CH_3) and 3.28 (s, 3H, N(1)-CH_3). ^{13}C NMR (125 MHz, DMSO-D_6, *δ*/ppm): 155.52 (>C=O), 150.54 (>C=N), 150.15 (>C=N), 143.77 (Ar-C), 140.18 (Ar-C), 127.43 (Ar-C), 119.06 (Ar-C), 30.65 (N-CH_3), 28.02 (N-CH_3). Anal. Calcd. for $C_{12}H_{12}N_6O_4S$: C, 42.85; H, 3.60; N, 24.99, Found: C, 43.03; H, 3.55; N, 25.09.

*2.3. Single crystal X-ray structure and refinement details for **AP2** and **AP4***

The intensity data were collected on a Bruker Kappa APEXII diffractometer equipped with a CCD area detector, employing MoKα radiation (λ = 0.71073 Å) and using graphite monochromator with ω scan. Crystal cell refinement and data reduction were carried out using Bruker SAINT-software package whereas absorption effects in the compound were corrected by using the Multi-Scan method (SADABS) [45]. The structural solution and refinement were carried out using the SHELXL-2014/7 suite of programs [46]. The structures were solved by employing direct methods or Patterson maps to locate the heavy atoms, followed by difference maps for the light, non-hydrogen atoms. All non-hydrogen atoms were refined with anisotropic thermal parameters. A summary of the crystallographic data collection and structure parameters for **AP2** and **AP4** is given in Table 1.

(Table 1)

2.4. *Topological analysis*

The H-bonded network in the structure of **AP4** was analyzed from the topological viewpoint by following the concept of the simplified underlying net [47,48]. Such a net was generated by contracting the molecular units to centroids, maintaining their connectivity via hydrogen bonds. Only strong D–H···A hydrogen bonds were considered, wherein the H···A <2.50 Å, D···A <3.50 Å, and ∠(D–H···A) >120°; D and A stand for donor and acceptor atoms [47].

3. Results and discussion

3.1. *Synthesis and structure*

The new derivatives of 8-azapurin-2,6-dione (*i.e.* 8-azaxanthines, Scheme 1C), 1,3-dimethyl-8-(aryl)-azapurin-2,6-diones (**AP1**-**AP4**), were synthesized by following an oxidation procedure in the presence of copper ions and in alkaline medium. The reaction mixture containing 1,3-dimethyl-5-(arylazo)-6-aminouracils (abbreviated as Uazo1-Uazo4), $NaHCO_3$ and $Cu(NO_3)_2 \cdot 3H_2O$ in DMF-water was treated at 70 °C with stirring for 1 h (see reaction in Scheme 2). The reactions were monitored by UV-vis spectroscopy as shown in Figure 1 (representative spectra for **AP2**). The Uazo compounds exist in anionic form of hydrazone in DMF; there is an H-bond between (λ_{max}= 369 nm for $Uazo2^-$, Figure 1a) of $Uazo^-$ and ^+HDMF [33a,e]. There is no remarkable band shifting occurs in the presence of base ($NaHCO_3$), also confirming an anionic form of hydrazone (λ_{max}= 369 nm for $Uazo2^-$, Figure 1b) [33a] in DMF. Upon addition of Cu(II) nitrate into the reaction mixture at heating condition, the absorption maximum (λ_{max} for $Uazo2^-$) shifts from 369 nm to 390 nm and a new weak band appears at 470 nm, indicating the formation of Cu(II)-complex with the Uazo2 (t = 0-5 min, Figure 1c) [49]. On further prolonging the heating, a new band is being developed at 315 nm; its intensity increases progressively with time. Simultaneously, the intensity at 390 nm decreases. The reaction is completed within 1 h. These data indicate that a new type of compounds has formed from Uazo substrates, specifically from Uazo Cu(II)-complexes, because the new band with a maximum at 315 nm is neither matched with the Uazo2 nor its copper(II) complex [49]. The products are the derivatives of 1,3-dimethyl-8-(aryl)-azapurin-2,6-diones. Based on the UV-vis data a mechanism of their formation is proposed and depicted in Scheme 3. The crystalline products (**AP1**-**AP4**) precipitated from the reaction mixture upon slow evaporation, and were then filtered off. The structures and spectroscopic properties of the compounds were established by studying them in the solid state (FT-IR and single crystal X-ray diffraction) and in solution (UV–vis and NMR spectroscopy).

(Scheme 2 and 3, Figure 1)

3.2. IR spectroscopic characterization

The IR data for all the compounds (**AP1**-**AP4**) are given in the experimental section. A representative IR spectrum for **AP3** along with its parent Uazo substrate, Uazo3 is shown in Figure 2 and rests are given in Figures S1-S3 (Supporting material). The IR spectra of **AP1**-**AP4** exhibit two sharp intense peaks at 1717 cm^{-1} and 1683 cm^{-1} (for **AP3**, Figure 2A) due to the carbonyl groups ($^{2}C=O$) and ($^{6}C=O$), respectively, in the uracil ring (see Scheme 2 for numbering). The peak positions are found red-shifted significantly in comparison with the parent Uazo compounds [33a] (Figure 2B). Another almost indistinguishable pair of sharp peaks at 1608 cm^{-1} and 1594 cm^{-1} is assigned to the ν(-C=N-) stretching frequencies; these peaks, as expected, are absent in the Uazo substrates (Figure 2B). The peaks at 1384 cm^{-1} and 1351 cm^{-1} belong to (-N-N-) group. In comparison with the spectrum of Uazo3 (Figure 2B) it is evident that the product is devoid of the –N=N– stretching frequency, supporting the formation of **AP3** from Uazo3. The IR study thus reveals that the products synthesized from Uazo compounds are devoid from the stretching frequencies of the azo-functionality and contain the –C=N- functions, thus providing an additional support toward the formation of 1,3-dimethyl-8-(aryl)-azapurin-2,6-diones (**AP1**-**AP4**).

(Figure 2)

*3.3. Crystal structures of **AP2** and **AP4** and topological analysis of **AP4***

The crystal structures of 1,3-dimethyl-8-(*p*-Me/SO_2NH_2-phenyl)-azapurin-2,6-dione (**AP2**/**AP4**) were solved to establish their solid state structures. Ellipsoid plots of **AP2** and **AP4** with atom labeling scheme are given in Figure 3 and 4, respectively. The bonding parameters about the triazole ring of the structures are listed in Table 2 and detail are given in Table S1, as supplementary material. The crystal of **AP2** consist twin molecular units (Figure 3) whereas **AP4** is single (Figure 4). In comparison with bond length data of the uracil moiety of Uazo4 **[**33e**]**, these are shortened in **AP4** as well as in **AP2**. The v-triazole ring is formed in the products under reaction condition by linking –NH2 group at 6-position of the uracil moiety with one of the azo-nitrogen, resulting –N-N- bond (Scheme 3). The newly formed –N-N- bond distance is found equivalent in molecule **B** of **AP2** (N(1)B-N(2)B) and **AP4** (N(1)-N(2)) (see Table 2) and in molecule **A** of **AP2** the distance is lengthened by 0.01 Å (N(1)A-N(2)A). As expected, in comparison with Uazo4 [33e], the N(1)-N(3) bond length increases by 0.014 Å and the C(7)-

N(3) bond distance decreases by 0.042 Å in **AP4**. Some anomaly is observed over the C(7)-C(8) (decreases by 0.042 Å) and C(8)-N(2) (increases by 0.014 Å) bond lengths. The N(1)-C(6) bond length in **AP4** remains similar to that of Uazo4. However, the C(7)-C(8) bond length is essentially identical to the -C-C- bond length of its phenyl ring, indicating the existence of a ring current within neighboring bonds. The increase of C(8)-N(2) bond length might be the cause of the formation of triazole ring *via* the N(2)-N(1) bonding (1.355 Å). The bond length data within the –N(1)-N(3)-C(7)-C(8)-N(2)-N(1)– ring thus suggest that Uazo4 converts to **AP4** *via* the formation of a triazole ring, having a ring current within the –N(3)-C(7)-C(8)-N(2)– bonds. Similar phenomenon about bond distances is observed in the molecular structure of **A** and **B** of **AP2** (Table 2). Nevertheless, the bond length values of uracil and triazole rings are essentially identical to those in 1,3-dimethyl-8-azaxanthine monohydrate [17]. The bond angles about triazole ring, especially C(7)-N(3)-N(1), N(3)-N(1)-N(2), and C(8)-N(2)-N(1) in **AP4** and similar in the molecular structure of **A** and **B** of **AP2** are also concomitant to those in 1,3-dimethyl-8-azaxanthine monohydrate [17]. The molecules of **AP2** and **AP4** are almost planar wherein three rings (uracil, triazole, and phenyl) are projected on a plane.

(Figure 3 and 4, Table 2)

In contrast to the molecular structures of **AP2**, the molecular structure of **AP4** exhibits H-bonded networks, mainly due to its potential H-bond acceptors and donors present in sulfonamide group. The H-bonding parameters for **AP4** are listed in Table 3. The structure of **AP4** is composed of the discrete 0D organic molecular units (Figure 4) that are assembled by two conventional N–H…O hydrogen bonds [N(6)-H(6B)...O(4) 3.122(4) Å; N(6)-H(6A)...O(2) 2.991(5) Å] to give a 1D H-bonded chain (Figure 5A). From the Figure 5A it is clearly seen that the sulfonamide groups of the molecular units are mainly involved in H-bonding interactions among themselves and act as 'self-molecular glue'. Of the two –NH groups of the sulfonamide group of a molecular unit, one acts as a single 'two-centered' and other one as a double 'three-centered' H-bond donor. Molecular units form self-assembled dimeric motifs in antiparallel fashion through two symmetrically related H-bonds involving uracil-O(4) and one –NH of the sulfonamide group. From the topological viewpoint, the resulting 1D H-bonded chains can be

classified as a uninodal 2-connected net with the 2C1 topology [47]. Interestingly, the adjacent chains are interdigitated to give a grid-like packing pattern along the *c* axis (Figure 5B).

(Table 3, Figure 5)

3.4. NMR spectroscopic characterization

The formation of **AP1**- **AP4** from Uazo substrates could also be confirmed by a comparative analysis of their ^{1}H NMR spectra in DMSO-D_6 with those of the parent Uazo compounds [33a, e]. The chemical shifts of different types of protons and carbons in the NMR spectra of the products are given in the experimental section. From comparison of the ^{1}H NMR spectra of **AP4** and Uazo4 (see Figure 6), it is quite apparent that the spectrum of **AP4** (Figure 6A) is completely devoid of signals corresponding to hydrazone (–NH-) and imine (=NH) moieties (these are present in the parent Uazo4 compound (Figure 6B) [33e]). The as-synthesized compounds **AP1**-**AP3** contain only the –N-CH_3, and Ar-H protons (see Figures S4, S6, S8) and including these **AP4** has additional –NH_2 protons of –SO_2NH_2 moiety. The protons of two –N-CH_3 groups appear as singlet at 3.28 and 3.49 ppm. The –SO_2NH_2 protons exhibit a singlet at 7.52 ppm at the spectrum of **AP4** (Figure 6A). The four aromatic protons show a doublet-doublet signal in the 8.02-8.27 ppm range. In comparison with the parent Uazo compounds, all the protons in **AP1**-**AP4** appear up-fielded, which may be the reason for the formation of a triazole ring. Thus, the NMR-study supports the formation of **AP1**-**AP4** products from their corresponding Uazos and its stability in solution. The ^{13}C NMR spectrum of **AP4** (a representative case) displays characteristic carbon signals at 155.52 ppm for two >C=O (uracil) and at 150.54 and 150.15 ppm for >C=N (triazole ring) functionalities. The peaks in the 143.77–119.06 ppm region (143.77, 140.18, 127.43, and 119.06 ppm) are due to aromatic carbon atoms. The signals at 30.65 and 28.02 ppm are assigned to the carbon signals of the N-CH_3 groups (uracil). However, peak values are quite different than that of Uazo4 [33e].

(Figure 6)

3.5. Absorption, excitation and emission behavior

The UV-vis, excitation and emission data for **AP1**- **AP4** were recorded in DMSO and DMF solution and are listed in Table 4. The absorption spectra of **AP1- AP4** are very different from those of their parent compounds, Uazo1-Uazo4. Figure 7A shows a representative example for **AP1** and Uazo1. The absorption maximum of **AP1** (λ_{max}, 313 nm in DMSO) is quite sharp and blue-shifted than that of Uazo1 (λ_{max}, 366 nm) in DMSO. Moreover, absorption maxima of all the products lie in the 311–322 nm range along with a weak broad peak centered at 386-392 nm in DMSO and DMF solvents. The former peak is attributed to $\pi \rightarrow \pi^*$ transitions whereas the later peak corresponds to $n \rightarrow \pi^*$ transitions. Resembling the absorption electronic transitions, the compounds also exhibit two excitation peaks in the corresponding emission spectra. These are 307 and 338 nm for **AP2** upon emission at 410 nm in DMSO. On the other hand, each compound, upon excitation at 330 nm, exhibits two emission peaks. For example, for **AP**2 these are 381 and 403 nm in DMSO (Figure 7B). Both excitation and emission spectra seem to follow mirror image rule and are symmetric in nature. The symmetric nature of these spectra result from the same electronic transitions are being involved in both excitation and emission and the similar vibrational energy levels of S_0 (singlet ground state) and S_1 (singlet first excited state).

(Table 4, Figure 7)

4. Conclusions

The difficulty in the synthesis of stable 8-substituted 8-azapurin derivatives could potentially be overcome by following the oxidation of 5-(arylazo)-6-aminouracil precursors using an alkaline copper sulfate/nitrate method. In the present work, we explored such a method by converting a series of four 1,3-dimethyl-5-(arylazo)-6-aminouracil substrates to novel 1,3-dimethyl-8-(aryl)-azapurin-2,6-dione derivatives **AP1- AP4**. The reactions proceed efficiently, in DMF-water medium, and result in good product yields and purity. The obtained products were fully characterized in solution and solid state by standard methods, revealing also the stability of the compounds in solution. Single crystals of 1,3-dimethyl-8-(*p*-Me/SO_2NH_2-phenyl)azapurin-2,6-dione (**AP2**/**AP4**) were also isolated and characterized by X-ray diffraction. An interesting feature of the crystal structure of **AP4** concerns the formation of 1D H-bonded chains that were topologically classified within the 2C1 type.

Given the presence of bioactive uracil and triazole moieties along with other functional groups in the structures of **AP1- AP4**, the obtained compounds may show promising biological or pharmacological properties, with a particular interest toward modelling new pharmaceutical agents. For the purposes, the molecule containing a bioactive sulphonamide group (**AP4**) can be particularly attractive. Further research toward the exploration of biological and/or pharmacological behaviour of these derivatives as well as the synthesis of an extended library of such organic compounds will be pursued.

Acknowledgements

The authors are thankful to Department of Chemistry, NIT Agartala, India for providing financial support and research facilities. We thank SAIF IIT Madras, for single crystal X-ray diffraction data for **AP4**. D.D. and A.P. greatly acknowledge NIT, Agartala for financial support. AMK acknowledges the FCT, Portugal (UID/QUI/00100/2013).

Appendix A. Supplementary material

CCDC number 1545458 and 1545459 contain the supplementary crystallographic data for the products, **AP2** and **AP4**, respectively. This data can be obtained free of charge *via* http://www.ccdc.cam.ac.uk/conts/retrieving.html, or from the Cambridge Crystallographic Data Centre, 12 Union Road, Cambridge CB2 1EZ, UK; fax: (+44) 1223-336-033; or e-mail: deposit@ccdc.cam.ac.uk.

Supplementary data includes IR spectra (Figures S1–S3), NMR spectra (Figures S4–S10) of **AP1**–**AP4** and bond lengths and angles for **AP2** and **AP4** (Table S1).

References

[1] B. Lippert, Coord. Chem. Rev. 200-202 (2000) 487.

[2] (a) M. S. Masoud and M. Y. A. El-Kaway, Spectrochim. Acta 102A (2013) 175; (b) M. S. Masoud, M. F. Amira, A. M. Ramadan, G. M. El-Ashry, Spectrochim. Acta 69A (2008) 230.

[3] A. Prabakaran and S. Muthu, Spectrochim. Acta 118A (2014) 578.

[4] S. –F. Qi, X. –N. Wang, Z. –Z. Yang, X. –H. Xu, J. Phys. Chem. B 113 (2009) 5645.

[5] M. W. Powner, J. D. Sutherland, J. W. Szostak, J. Am. Chem. Soc. 132 (2010) 16677.

[6] A. Albert, Adv, Heterocycl. Chem. 39 (1986) 117.

[7] C.R. Maldonado, M. Quiros, J.M. Salas, Polyhedron 28 (2009) 911.

[8] C.R. Maldonado, M. Quiros, J.M. Salas, A. Rodríguez-Diéguez, Inorg. Chim. Acta 362 (2009) 1553.

[9] V. Ravichandran, G.A. Ruban, K.K. Chacko, M.A.R. Molina Rodríguez, E.C.J.M. Salas-Peregrín, K. Aoki, H. Yamazaki, J. Chem. Soc., Chem. Commun. (1986) 1780–1782.

[10] L.G. Purnell, E.D. Estes, D.J. Hodgson, J. Am. Chem. Soc. 98 (1976) 740.

[11] B.J. Graves, D.J. Hodgson, Inorg. Chem. 20 (1981) 2223.

[12] J. Gu, J. Wang, J. Leszcynski, J. Am. Chem. Soc. 126 (2004) 12651.

[13] M. E. García-Rubiño, M. C. Núñez-Carretero, D. Choquesillo-Lazarte, J. M. García-Ruiz, Y. Madrid, J. M. Campos, RSC Adv. 4 (2014) 22425.

[14] M. Abdoli, Z. Mirjafary, H. Saeidian, A. Kakanejadifard, RSC. Adv. 5 (2015) 44371.

[15] L. Zhou, H. Zhang, S. Tao, M. Ehteshami, J. H. Cho, T. R. McBrayer, P. Tharnish, T. Whitaker, F. Amblard, S. J. Coats, R. F. Schinazi, ACS Med. Chem. Lett. 7 (2016) 17.

[16] C. Li and F. Zhang, Tetrahedron Lett. 58 (2017)1572.

[17] M. P. Sánchez, M. A. Romero, J. M. Salas, D. J. Cárdenas, J. Molina, M. Quirós, J. Mol. Struc. 344 (1995) 257-264.

[18] (a) C. J. Coulson, R. E. Ford, E. Lunt, S. Marshall, D.L. Pain, J. H. Rogers, K.R. Wooldridge, Eur. J. Med. Chem. 9 (1974) 313; (b) P. Franchetti, L. Messini, L. Cappellacci, M. Grifantini, A. Lucacchini, C. Martini, G. Senatore, J. Med. Chem. 37 (1994) 2970; (c) L. Havlicek, K. Fuksova, V. Krystof, M. Orsag, B. Vojtesek, M. Strnad, Bioorg. Med. Chem. 13 (2005) 5399; (d) I. Giorgi, A.M. Bianucci, G. Biagi, O. Livi, V. Scartoni, M. Leonardi, D. Pietra, A. Coi, I. Massarelli, F.A. Nofal, F.L. Fiamingo, P. Anastasi, G. Giannini, Eur. J.

Med. Chem. 42 (2007) 1; (e) J. Wierzchowski, J. M. Antosiewicz, D. Shugar, Mol. BioSyst. 10 (2014) 2756.

[19] (a) W.S. Sheldrick, G. Heeb, Inorg. Chim. Acta 190 (1991) 241; (b) D. Chuan, D. Li-hua, W. Yu-xia, L. Jun-fen, W. Yan-li, Spectrochim. Acta 59A (2003) 3131.

[20] W. Traube, Ber. Dtsch. Chem. Ges. 33 (1900) 3056.

[21] J. J. Fox and D. van Praag, J. Am. Chem. Soc. 26 (1961) 526.

[22] T. Kishikawo and H. Yuki, Chem. Pharm. Bull.14 (1966) 1365; (b) M. Ridi, G. Franchi, S. Mangiavacchi, M. P. Lombardini, Boll.Chim.Farm.107 (1968) 401.

[23] R. Islam and T. Nagamatsu, Synthesis (2006) 4167.

[24] D. A. Babkov, A. N. Geisman, A. L. Khandazhinskaya, M. S. Novikov, Russ. Chem. Rev. 38 (2016) 308 and references therein.

[25] A. Albert, J. Chem. Soc. B (1966) 427.

[26] G. Nubel and W. Pfleiderer, Chem. Ber. 98 (1965) 1060.

[27] (a) A. Albert, J. Chem. Soc. C (1968) 2076; (b) A. Albert and K. Tratt, J. Chem. Soc. C (1968) 344.

[28] G. M. Ziarani, N. H. Nasab, N. Lashgari, RSC Adv. 6 (2016) 38827.

[29] (a) A. A. Mustafa, A. A. Alhaider, A. A. Hijazi, Pharm. Res. 6 (1989) 394; (b) C. Bayrak, J. Biol. Chem. 40 (2012) 419.

[30] V.M. Nesterov, L.A. Kucherya, L.A. Tretyakova, L.I. Markitantova, Phar. Chem. J. 15 (1981) 591.

[31] C.D. Mol, A.S. Arvai, G. Slupphaug, B. Kavli, I. Alseth, H. E. Krokan, J. Tainer, Cell 80 (1995) 869.

[32] D. Dobritzsch, G. Schneider, K. Schnackerz, Y. Lindqvist, The EMBO J. 20 (2001) 650.

[33] (a) D. Debnath, S. Roy, B. –H. Li, C. –H. Lin, T. K. Misra, Spectrochim. Acta 140A (2015) 185; (b) D. Debnath, A. Purkayastha, R. Choudhury, T. K. Misra, J. Chin. Chem. Soc. 63 (2016) 580; (c) D. Debnath, A. Purkayastha, R. Choudhury, T. K. Misra, Ind. Chem. Soc. 93 (2016) 989-998; (d) A. Purkayastha, D. Debnath, S. Roy, A. Bauzá, R. Choudhury, A. Frontera, T. K. Misra, Eur. J. Inorg. Chem. 36 (2016) 5585; (e) D. Debnath, S. Roy, A. Purkayastha, A. Bauzá, R. Choudhury, R. Ganguly, A. Frontera, T. K. Misra, J. Mol. Struct. 1141 (2017) 225.

[34] F. R. Benson, L. W. Hartzel, W. L. Savell, J. Am. Chem. Soc. 72 (1950) 1816 and references therein.

[35] Y. Maki and E. C. Taylor, Chem. Pharm. Bull. 20 (1972) 605.

[36] R. Islam and T. Nagamatsu, Heterocycles 68 (2006) 2387.

[37] C. Hansch, P. G. Sammes, J. B. Taylor, Comprehensive Medicinal Chemistry, Vol. 2, Pergamon Press: Oxford 1990, Chap. 7.1.

[38] D. Vullo, V. De Luca, A. Scozzafava, V. Carginale, M. Rossi, C. T. Supuran, C. Capasso, Bioorg. Med. Chem. 21 (2013) 4521.

[39] T. Ma, A. D. Fuld, J. R. Rigas, A. E. Hagey, G. B. Gordon, E. Dmitrovsky, K. H. Dragnev, Chemotherapy 58 (2012) 321.

[40] S. Terada, K. Katagiri, H. Masu, H. Danjo, Y. Sei, M. Kawahata, M. Tominaga, K. Yamaguchi, I. Azumaya, Cryst. Growth Des. 12 (2012) 2908.

[41] (a) K. Katagiri, T. Ikeda, M. Tominaga, H. Masu, I. Azumaya, Cryst. Growth Des. 10 (2010) 2291; (b) A. Zoppi, M. A. Quevedo, A. Delrivo, M. R. Longhi, J. Pharm. Sci. 99 (2010) 3166.

[42] (a) M. R. Caira, Mol. Pharm. 4 (2007) 310; (b) N. R. Goud, S. Gangavaram, K. Suresh, S. Pal, S. G. Manjunatha, S. Nambiar, A. Nangia, J. Pharm. Sci. 101 (2012) 664; (c) S. Ghosh, P. P. Bag, C. M. Reddy, Cryst. Growth Des. 11 (2011) 3489.

[43] (a) A. L. Bingham, D. S. Hughes, M. B. Hursthouse, R. W. Lancaster, S. Tavener, T. L. Threlfall, Chem. Commun. (2001) 603; (b) S. Aitipamula, P. S. Chow, R. B. H. Tan, CrystEngComm 14 (2012) 691; (c) J. Pratt, J. Hutchinson, C. L. Klein Stevens, Acta Crystallogr. 67C (2011) 0487.

[44] Z. -Q. Hu, C. -F. Chen, Chem. Commun. (2005) 2445.

[45] Sheldrick GM, *SADABS V2014/4* (Bruker AXS Inc.), University of Göttingen, Göttingen, Germany, 2014.

[46] *SHELXTL-2014/7 (Sheldrick, 2014)*, Bruker AXS Inc., Madison, WI, USA, 2014.

[47] V. A. Blatov, IUCr CompComm Newsletter, 2006, no 7, 4-38.

[48] V. A. Blatov, A. P. Shevchenko, D. M. Proserpio, Cryst. Growth Des. 14 (2014) 3576.

[49] E. Colacio, J. –P. Costes, R. Kivekäs, J. –P. Laurent, J. Ruiz, M. Sundberg, Inorg. Chem., 30 (1991) 1475.

Legends to Scheme, Figures and Tables

Schemes

Scheme 1. Molecular structures of purine derivatives (**A**-**D**).

Scheme 2. A general reaction scheme for the synthesis of 1,3-dimethyl-8-(aryl)azapurin-2,6-diones (**AP1**-**AP4**).

Scheme 3. Plausible mechanistic paths for the conversion of 1,3-dimethyl-5-(arylazo)-6-aminouracils (Uazo1–Uazo4) to 1,3-dimethyl-8-(aryl)-azapurin-2,6-diones (**AP1**–**AP4**).

Figures

Figure 1. UV-vis spectra of intermediate products (**a**, **b**) and of the reaction mixture in the course of the formation of the **AP2** product (**c**) with 5 min time-intervals for 1h.

Figure 2. IR spectra of (**A**) 1,3-dimethyl-8-(*p*-Cl-phenyl)-azapurin-2,6-dione (**AP3**) and (**B**) 1,3-dimethyl-5-(*p*-Cl-phenylazo)-6-aminouracil (Uazo3).

Figure 3. Molecular view of **AP2** with atom labelling scheme and 40% probability thermal ellipsoids.

Figure 4. Molecular view of **AP4** with atom labelling scheme and 40% probability thermal ellipsoids.

Figure 5. Structural fragments of **AP4**. (**A**) 1D H-bonded chain (H-bonds are shown as dashed lines. (**B**) Topological representation of an underlying 1D H-bonded network showing a packing arrangement of uninodal 2-connected chains with the 2C1 topology. Further details: (**A**): color codes: C (pale green), O (red), N (blue), S (yellow), H (gray); (**B**) centroids of 2-connected molecular nodes (pale green balls), view along the *c* axis.

Figure 6. ^{1}H NMR spectra of: (**A**) the as-synthesized **AP4** product and (**B**) the Uazo4 precursor.

Figure 7. (**A**) UV-vis spectra of Uazo1 and **AP1** in DMSO. (**B**) Excitation and emission spectra of (**a**) **AP1**, (**b**) **AP2**, (**c**) **AP3**, and (**d**) **AP4**.

Tables

Table 1. Crystallographic data and structure refinement of **AP2** and **AP4**

Empirical formula	**$C_{13}H_{13}N_5O_2$(AP2)**	**$C_{12}H_{12}N_6O_4S$ (AP4)**
Formula weight	271.28	336.34
Temperature/K	296(2)	293(2)
Crystal system	Triclinic	Monoclinic
Space group	P-1	$P2_1/c$
a/Å	7.1521(14)	12.6717(6)
b/Å	12.613(3)	8.9385(4)
c/Å	14.782(3)	13.2445(7)
α/°	88.151(6)	90
β/°	84.146(6)	113.366(3)
γ/°	74.766(6)	90
Volume/$Å^3$	1279.9(4)	1377.12(12)
Z	4	4
$\rho_{calcM}g/m^3$	1.408	1.622
μ/mm^{-1}	0.100	0.269
F(000)	568.0	696
Crystal size/mm^3	0.320 × 0.120 × 0.040	0.350 x 0.300 x 0.250
2θ range for data collection/°	5.94 to 52.94	2.828 to 24.998
Index ranges	$-8 \le h \le 8$, $-15 \le k \le 15$, $-18 \le l \le 18$	-15<=h<=15, -10<=k<=10, -15<=l<=15
Reflections collected	31252	26166
Independent reflections	5215 [R_{int} = 0.1214, R_{sigma} = 0.0729]	2413 [R(int) = 0.0713]
Data/restraints/parameters	5215/0/367	2413 / 3 / 216
Goodness-of-fit on F^2	1.085	1.055
Final R indexes [$I \ge 2\sigma$ (I)]	R_1 = 0.0972, wR_2 = 0.2560	R1 = 0.0459, wR2 = 0.0977
Final R indexes [all data]	R_1 = 0.1573, wR_2 = 0.3153	R1 = 0.0826, wR2 = 0.1186
Largest diff. peak/hole / e $Å^{-3}$	0.43/-0.30	0.326 and -0.302

Table 2. Selected bond lengths (Å) and angles (º) of compound **AP2** and **AP4** in and around triazole ring.

Compound AP2				Compound AP4	
Molecule A		**Molecule B**			
Bonds	**Bond length (Å)**	**Bonds**	**Bond length (Å)**	**Bonds**	**Bond length (Å)**
C(1)A-C(2)A	1.379(6)	C(1)B-C(2)B	1.381(6)	N(1)-N(2)	1.355(3)
C(2)A-C(3)A	1.428(6)	C(2)B-C(3)B	1.421(6)	N(1)-N(3)	1.324(3)
C(1)A-N(5)A	1.370(5)	C(1)B-N(5)B	1.377(5)	C(7)-N(3)	1.337(4)
C(1)A-N(1)A	1.325(5)	C(1)B-N(1)B	1.325(5)	C(7)-C(8)	1.376(4)
N(1)A-N(2)A	1.361(4)	N(1)B-N(2)B	1.354(5)	C(8)-N(2)	1.327(4)
N(2)A-N(3)A	1.330(5)	N(2)B-N(3)B	1.324(5)	C(6)-N(1)	1.422(4)
C(2)A-N(3)A	1.348(5)	C(2)B-N(3)B	1.348(5)	C(8)-N(4)	1.367(4)
C(7)A-N(2)A	1.416(5)	C(7)B-N(2)B	1.438(5)	C(7)-C(10)	1.436(4)
C(7)A-C(8)A	1.382(6)	C(7)B-C(8)B	1.366(6)	C(1)-C(6)	1.383(4)
C(7)A-C(13)A	1.377(6)	C(7)B-C(13)B	1.378(6)	C(5)-C(6)	1.388(4)
Bonds	**Bond angles (º)**	**Bonds**	**Bond angles (º)**	**Bonds**	**Bond angles (º)**
N(1)A-C(1)A-N(5)A	125.5(4)	N(1)B-C(1)B-N(5)B	127.0(4)	N(3)-N(1)-C(6)	121.9(2)
N(5)A-C(1)A-C(2)A	122.9(4)	N(5)B-C(1)B-C(2)B	121.7(4)	N(2)-N(1)-C(6)	121.8(2)
N(3)A-C(2)A-C(3)A	129.7(4)	N(3)B-C(2)B-C(3)B	130.1(4)	C(8)-N(2)-N(1)	101.6(2)
C(13)A-C(7)A-C(8)A	120.8(4)	C(8)B-C(7)B-C(13)B	120.1(4)	N(1)-N(3)-C(7)	102.6(2)
C(8)A-C(7)A-N(2)A	119.5(4)	C(13)B-C(7)B-N(2)B	120.2(4)	N(3)-N(1)-N(2)	116.4(2)
N(1)A-C(1)A-C(2)A	111.6(4)	N(1)B-C(1)B-C(2)B	111.2(4)	N(3)-C(7)-C(10)	128.2(3)
N(3)A-C(2)A-C(1)A	108.4(4)	N(3)B-C(2)B-C(1)B	107.9(4)	C(8)-C(7)-C(10)	122.5(3)
C(1)A-C(2)A-C(3)A	121.9(4)	C(1)B-C(2)B-C(3)B	122.0(4)	N(2)-C(8)-N(4)	127.2(3)
C(13)A-C(7)A-N(2)A	119.7(4)	C(8)B-C(7)B-N(2)B	119.7(4)	N(2)-C(8)-C(7)	110.3(3)
C(1)A-N(1)A-N(2)A	100.8(3)	C(1)B-N(1)B-N(2)B	101.4(3)	N(4)-C(8)-C(7)	122.5(3)
N(3)A-N(2)A-C(7)A	122.4(3)	N(3)B-N(2)B-C(7)B	121.3(3)	C(1)-C(6)-C(5)	121.4(3)
N(2)A-N(3)A-C(2)A	102.4(3)	N(2)B-N(3)B-C(2)B	103.1(3)	C(1)-C(6)-N(1)	119.8(3)
N(3)A-N(2)A-N(1)A	116.8(3)	N(3)B-N(2)B-N(1)B	116.4(3)	C(5)-C(6)-N(1)	118.8(3)
N(1)A-N(2)A-C(7)A	120.8(3)	N(1)B-N(2)B-C(7)B	122.4(3)	N(3)-C(7)-C(8)	109.2(3)

Table 3. Hydrogen bonding parameters for **AP4** [Å and (°)].

D-H...A	d(D-H)	d(H...A)	d(D...A)	<(DHA)
N(6)-H(6B)...O(1)#5	0.812(18)	2.58(4)	3.146(4)	128(3)
N(6)-H(6B)...O(4)#6	0.812(18)	2.50(3)	3.122(4)	135(4)
N(6)-H(6A)...O(2)#7	0.819(17)	2.180(18)	2.991(5)	171(3)
C(1)-H(1)...O(2)#1	0.93	2.58	3.302(4)	134.3
C(4)-H(4)...O(3)#2	0.93	2.63	3.153(4)	116.4
C(5)-H(5)...O(3)#2	0.93	2.36	3.017(4)	127.8
C(12)-H(12A)...O(1)#3	0.96	2.44	3.209(4)	136.7
C(12)-H(12C)...N(3)#4	0.96	2.59	3.542(4)	171.4

Symmetry transformations used to generate equivalent atoms:
#1 -x+1,-y+1,-z ; #2 x,y+1,z ; #3 x+1,-y+1/2,z+1/2 ; #4 -x+2,-y,-z; #5 -x+1,y+1/2,-z-1/2; #6 -x+2,-y+1,-z; #7 -x+1,-y+2,-z

Table 4. UV-vis, excitation and emission data of **AP1-AP4**

Compd.	**UV-Vis**		**Excitation and Emission**			
	DMF	**DMSO**	**DMF**		**DMSO**	
	λ_{max}, nm	**λ_{max}, nm**	**λ_{ex}, nm**	**λ_{em}, nm**	**λ_{ex}, nm**	**λ_{em}, nm**
AP1	311, 386	313, 386	304, 334	376, 404	304, 334	376, 405
AP2	315, 388	318, 388	306, 338	381, 403	307, 338	381, 403
AP3	316, 390	317, 390	307, 338	379, 404	306, 338	379, 400
AP4	320, 392	322, 392	308, 344	379, 405	307, 343	380, 405

Figure 1

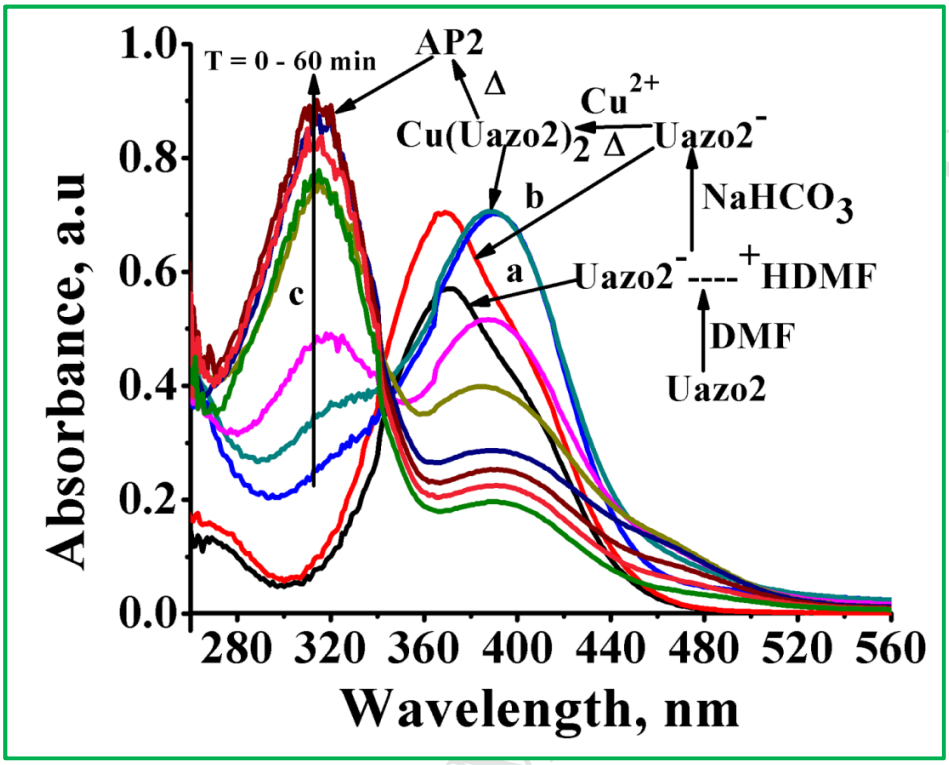

Figure 1. UV-vis spectra of intermediate products (**a**, **b**) and of the reaction mixture in the course of the formation of the **AP2** product (**c**) with 5 min time-intervals for 1h.

Figure 2

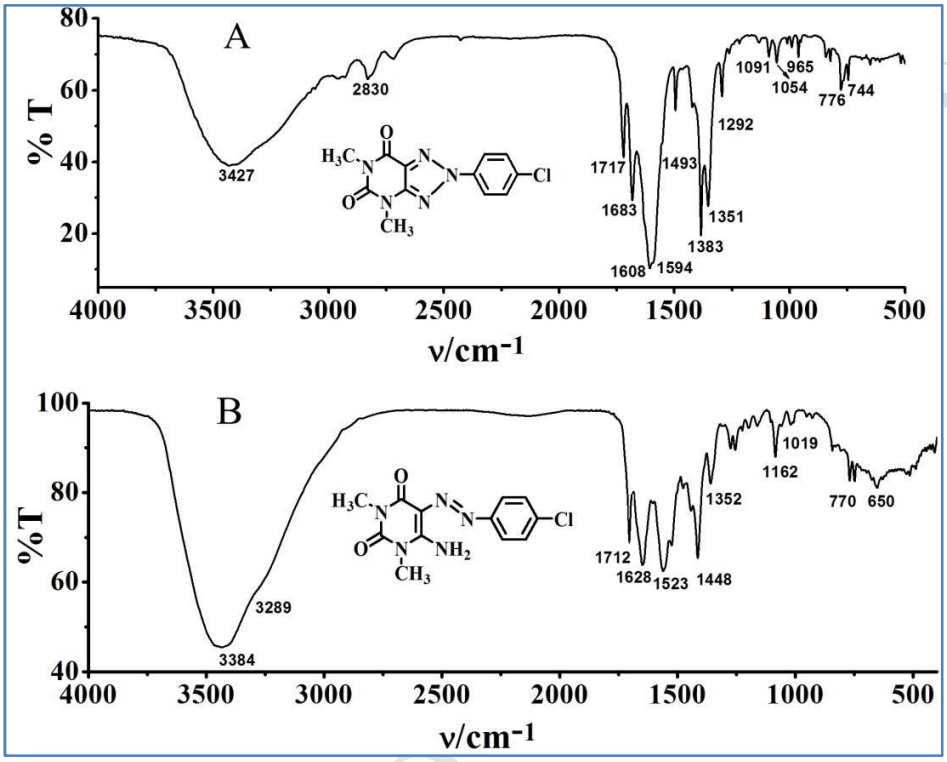

Figure 2. IR spectra of (**A**) 1,3-dimethyl-8-(*p*-Cl-phenyl)-azapurin-2,6-dione (**AP3**) and (**B**) 1,3-dimethyl-5-(*p*-Cl-phenylazo)-6-aminouracil (Uazo3).

Figure 3

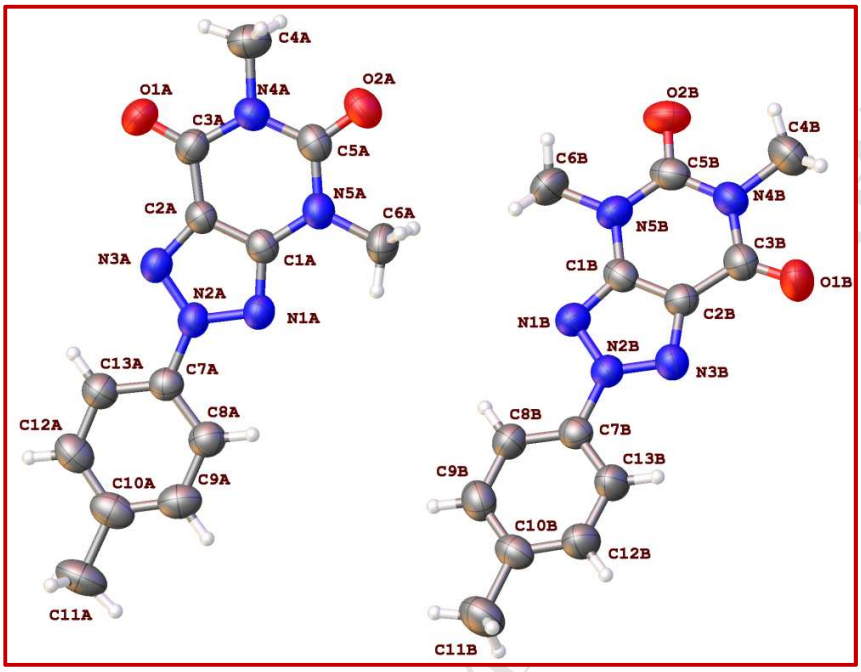

Figure 3. Molecular view of **AP2** with atom labelling scheme and 40% probability thermal ellipsoids.

Figure 4

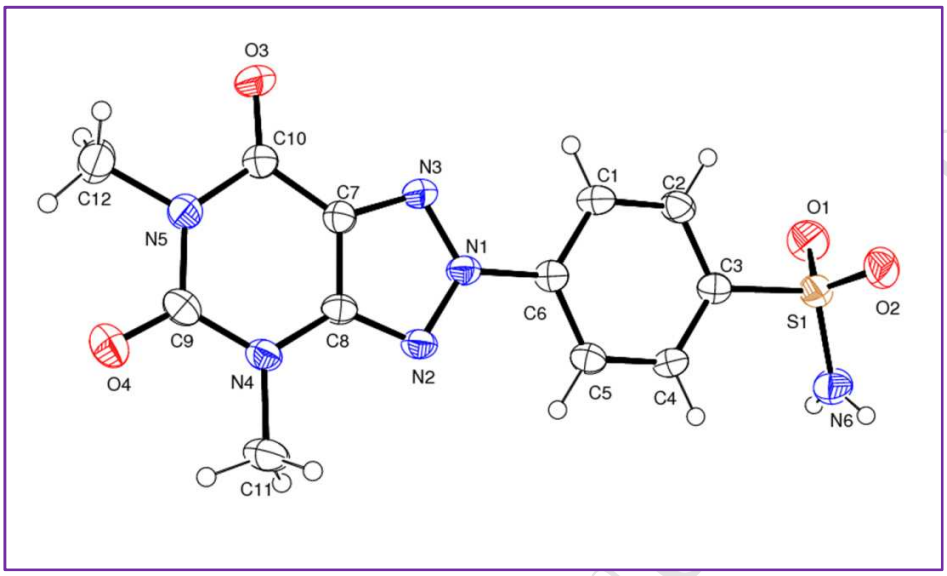

Figure 4. Molecular view of **AP4** with atom labelling scheme and 40% probability thermal ellipsoids.

Figure 5

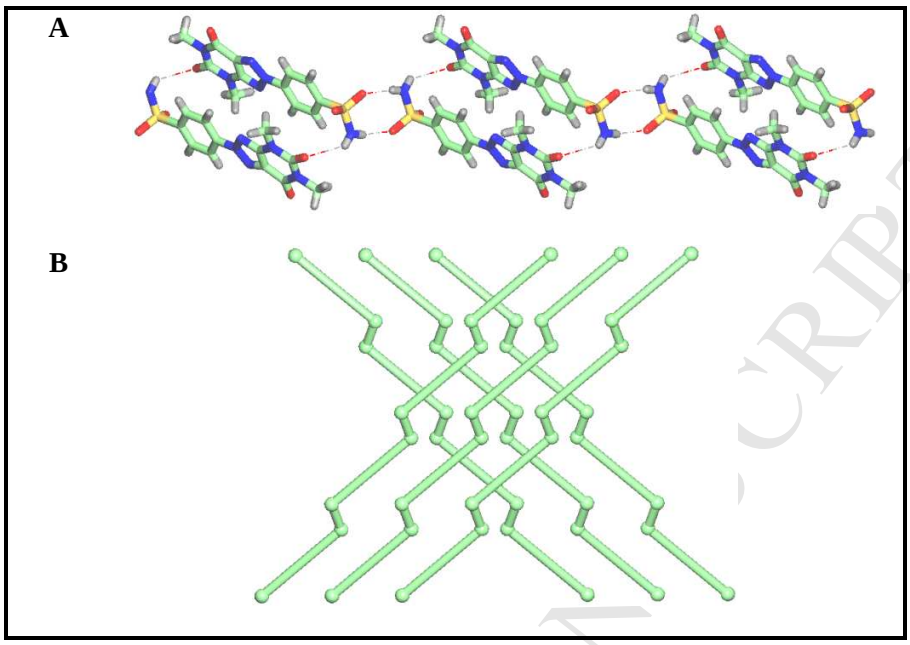

Figure 5. Structural fragments of **AP4**. (**A**) 1D H-bonded chain (H-bonds are shown as dashed lines. (**B**) Topological representation of an underlying 1D H-bonded network showing a packing arrangement of uninodal 2-connected chains with the 2C1 topology. Further details: (**A**): color codes: C (pale green), O (red), N (blue), S (yellow), H (gray); (**B**) centroids of 2-connected molecular nodes (pale green balls), view along the *c* axis.

Figure 6

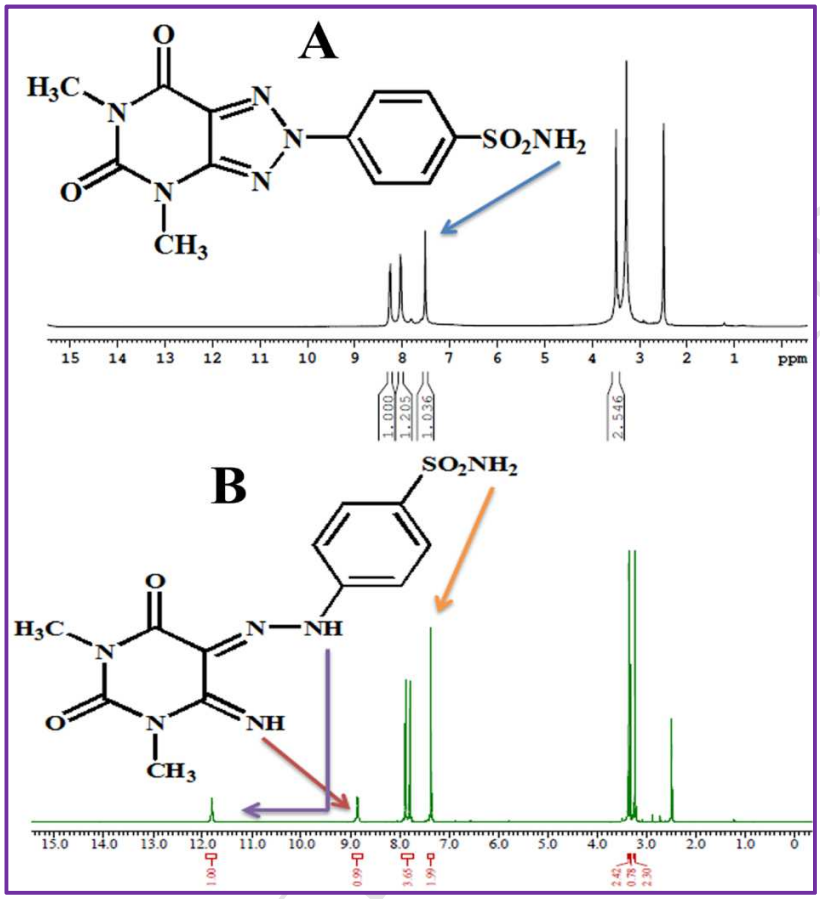

Figure 6. ^{1}H NMR spectra of: (**A**) the as-synthesized **AP4** product and (**B**) the Uazo4 precursor.

Figure 7

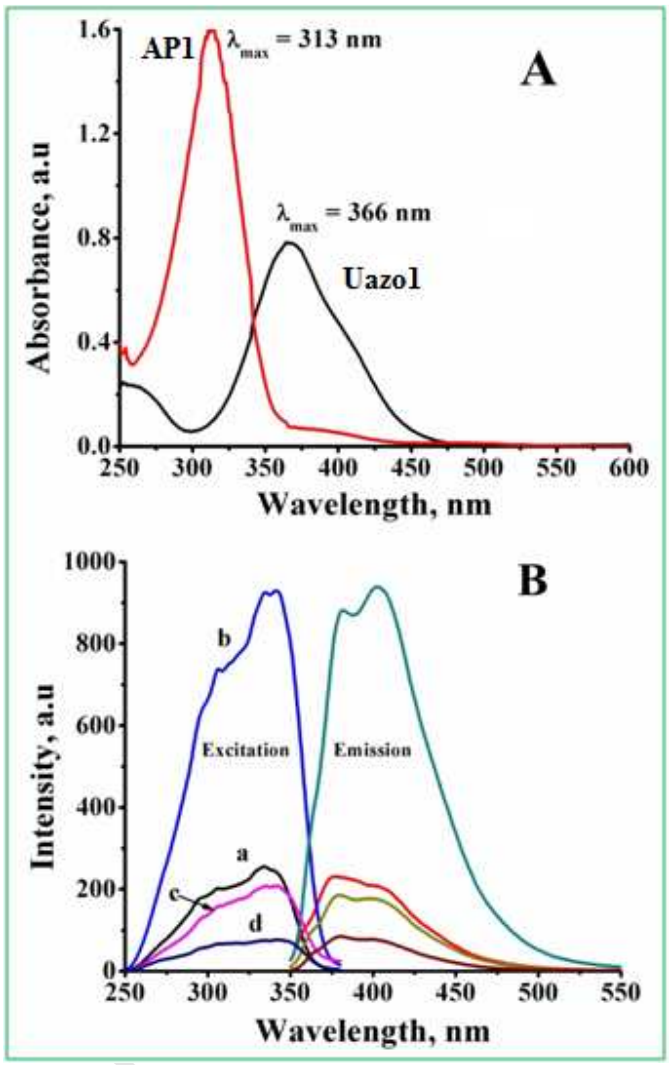

Figure 7. (**A**) UV-vis spectra of **Uazo1** and **AP1** in DMSO. (**B**) Excitation and emission spectra of (**a**) **AP1**, (**b) AP2**, (**c**) **AP3**, (**d**) **AP4**.

Schemes

Scheme 1

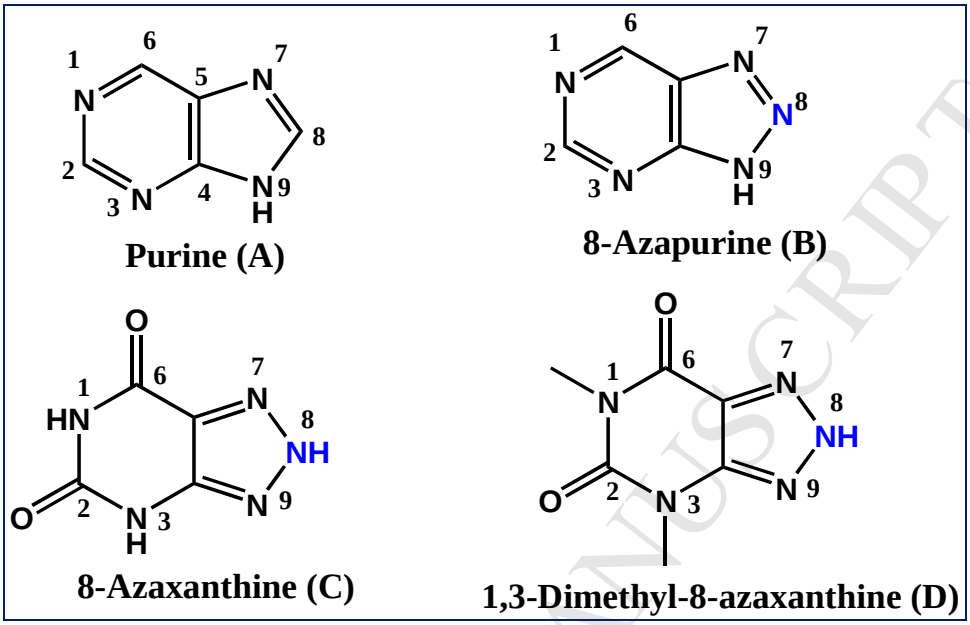

Scheme 1. Molecular structures of purine derivatives.

Scheme 2

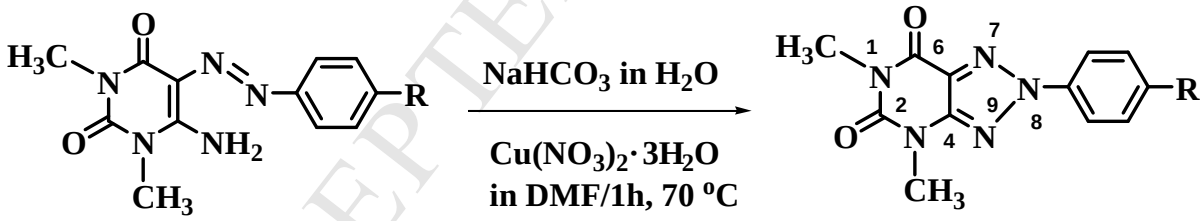

R = H; Uazo1
R = CH_3; Uazo2
R = Cl; Uazo3
R = SO_2NH_2; Uazo4

R = H; AP1
R = CH_3; AP2
R = Cl; AP3
R = SO_2NH_2; AP4

Scheme 2. A general reaction scheme of synthesis of 1,3-dimethyl-8-(aryl)-azapurin-2,6-dione (**AP1**-**AP4**).

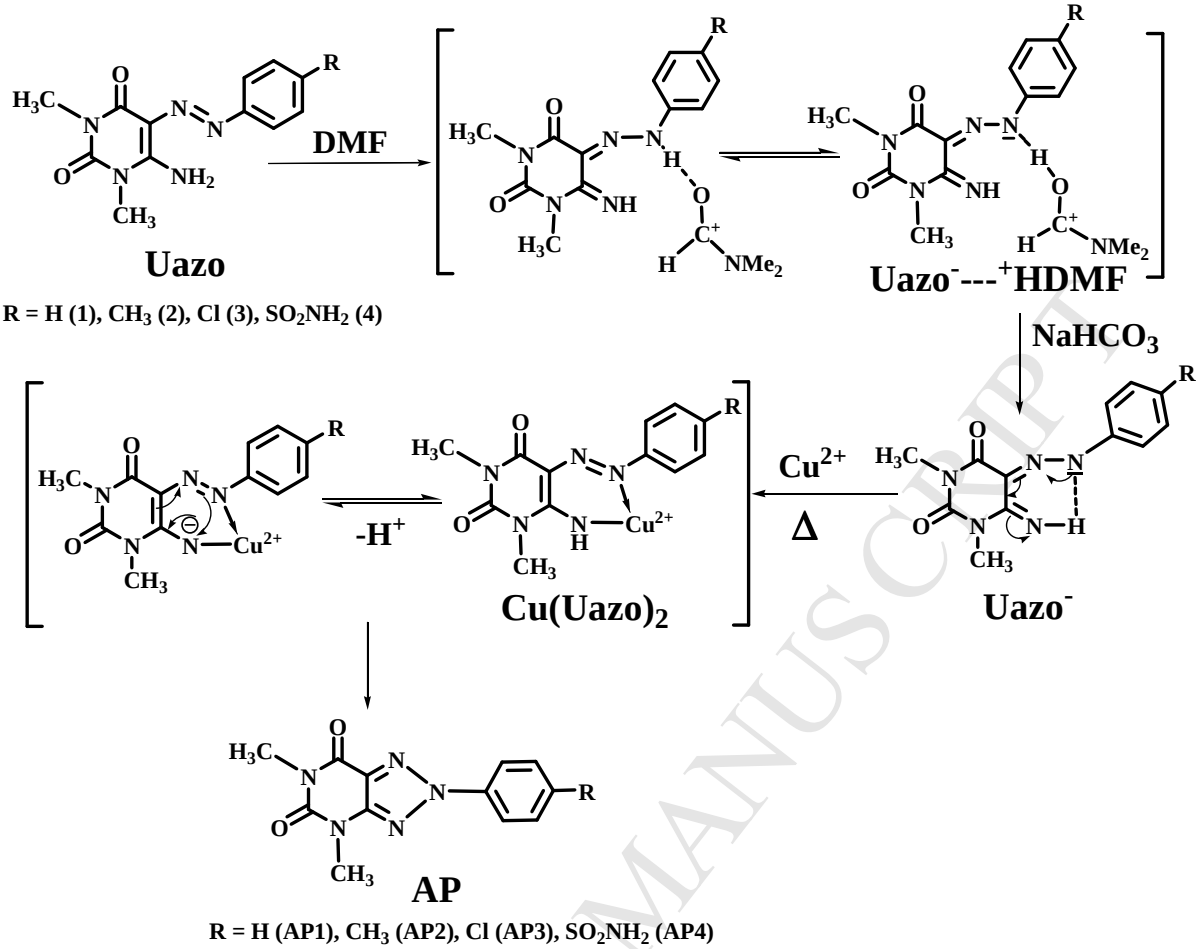

Scheme 3. Plausible mechanistic paths for the conversion of 1,3-dimethyl-5-(arylazo)-6-aminouracils (Uazo1–Uazo4) to 1,3-dimethyl-8-(aryl)azapurin-2,6-diones (**AP1**–**AP4**).

Highlights

- Reactivity of 1,3-dimethyl-5-(arylazo)-6-aminouracils
- Synthesis of 1,3-dimethyl-8-(aryl)-azapurin-2,6-diones.
- Structures of 1,3-dimethyl-8-(*p*-Me/SO_2NH_2-C_6H_4)-azapurin-2,6-diones
- Elucidation of solution state structures
- UV-vis, excitation and emission spectroscopy.